Supporting Information

Experimental Assignment of Long-Range Magnetic Communication Through Pd & Pt Metallophilic Contacts

Emil M. H. Larsen,[‡a] Niels A. Bonde,[‡a,b] Høgni Weihe,[a] Jacques Ollivier,[b] Tom Vosch,[a] Thomas Lohmiller,[c,d] Karsten Holldack,[f] Alexander Schnegg,[d,e] Mauro Perfetti,[f] and Jesper Bendix*[a]

* *Corresponding Author.*

Contents

[0]† Electronic supplementary information (ESI) available: Experimentals, crystallographic details(CCDC 2207828-2207833), Computational data, INS data, FD-FT THz-EPR data. For ESI and crystallographic data in CIF or other electronic format see DOI: 00.0000/00000000.

[0]‡ These authors contributed equally to this work.

[0a] *Department of Chemistry, University of Copenhagen, Universitetsparken 5, DK-2100 Copenhagen, Denmark.*

[0b] *Institut Laue-Langevin, 71 avenue des Martyrs, CS 20156, 38042 Grenoble Cedex 9, France*

[0c] *Humboldt-Universität zu Berlin, Institut für Chemie, Brook-Taylor-Str. 2, 12489 Berlin, Germany*

[0d] *EPR4Energy Joint Lab, Department Spins in Energy Conversion and Quantum Information Science, Helmholtz Zentrum Berlin für Materialien und Energie GmbH, Albert-Einstein-Straße 15, 12489 Berlin, Germany*

[0e] *Max Planck Institute for Chemical Energy Conversion, Stiftstrasse 34-36, D-45470 Mülheim an der Ruhr, Germany*

[0f] *Department of Optics and Beamlines, Helmholtz Zentrum Berlin für Materialien und Energie GmbH, Albert-Einstein-Straße 15, 12489 Berlin, Germany*

[0g] *Department of Chemistry "U. Schiff", University of Florence, Via della Lastruccia 3-13, Sesto Fiorentino, 50019, Italy*

1 Experimentals

[Co(Pd(SAc)$_4$)(OH$_2$)] 172 mg (1.51 mmol) KSAc was dissolved in 2 ml water. To this a solution of 100 mg (0.340 mmol) $Na_2[PdCl_4]$ in 2 ml water was added dropwise at a rate so that no permanent brown precipitate was observed, and was then left stirring for 30 min. A solution 80.8 mg (0.340 mmol) $CoCl_2 \cdot 6\,H_2O$ was added in a minimal amount of water and a green powder immediately precipitated. The green powder was isolated and dried briefly on a sintered glass funnel. Yield: 43 % based on Pd. Elemental analysis calculated for $PdCoC_8H_{14}O_5S_4$: C; 19.9 %, H; 2.92 %, N; 0.00 %. Found: C; 19.6 %, H; 3.15 %, N; 0.00 %.

[Ni(Pd(Sac)$_4$)(OH$_2$)] was obtained in a similar fashion to **[Co(Pd(SAc)$_4$)(OH$_2$)]**: $CoCl_2 \cdot 6\,H_2O$ was replaced with $NiCl_2 \cdot 6\,H_2O$ and the precipitate was of a yellow color. Yield: 65 % based on Pd. Elemental analysis calculated for $PdNiC_8H_{14}O_5S_4$: C; 19.9 %, H; 2.92 %, N; 0.00 %. Found: C; 19.5 %, H; 3.20 %, N; 0.00 %.

[Co(Pt(SAc)$_4$)(OH$_2$)] was obtained with a modification of the synthetic procedure reported[1] 100 mg (0.963 mmol) KSAc was dissolved in 30 ml water and to this a solution of 100 mg (0.241 mmol), $K_2[PtCl_4]$ in 3 ml water was added dropwise. The solution was stirred for 1.5 hour. To the resulting yellow solution 57.3 mg (0.241 mmol), $CoCl_2 \cdot 6\,H_2O$ dissolved in 3 ml water was added, and a gray powder immediately precipitated. The suspension was left at 5 °C overnight, where the particle size increased significantly. The powder was isolated and dried on a sintered glass funnel. Yield: 35 % based on Pt.

[Ni(Pt(SAc)$_4$)(OH$_2$)] was obtained in a similar fashion to [Co(Pt(SAc)$_4$)(OH$_2$)] where $CoCl_2 \cdot 6\,H_2O$ was replaced with $NiCl_2 \cdot 6\,H_2O$. The resulting precipitate was yellow in color and was isolated via centrifugation rather than filtration and dried under a stream of N_2. Yield: 80 % based on Pt.

[Co(Pd(SAc)$_4$)(pyNO$_2$)]$_2$, **{CoPd}$_2$**, 92.1 mg (0.146 mmol) [CoPd(SAc)4(OH2)] was suspended in 4 ml CH_2Cl_2, and dropwised added a solution of 18.1 mg (0.146 mmol) 3-nitropyridine in a minimal amount of CH_2Cl_2. Upon addition of the 3-nitropyridine the remaining precipitate was dissolved, and while stirring for 24 hours the solution changed color from green to dark yellow. Crystals suitable for X-ray diffraction experiments were grown by slow evaporation of the resulting solution at room temperature. Yield: 56 % based on Pd. Elemental analysis calculated for $Pd_2Co_2C_{26}H_{32}N_4O_{12}S_8$: C; 26.5 %, H; 2.73 %, N; 4.75 %. Found: C; 26.5 %, H; 2.71 %, N; 4.81 %.

[Ni(Pd(SAc)$_4$)(pyNO$_2$)]$_2$, **{NiPd}$_2$**, 33.0 mg (0.0682 mmol) of [Ni(Pd(SAc)$_4$)(OH$_2$)] was dissovled in 1 ml CH_2Cl_2, followed by dropwise addition of a solution of 8.47 mg (0.0682 mmol) 3-nitropyridine in a minimal amount of CH_2Cl_2. The solution was stirred for 1 hour during which the solution changed color from yellow to green. The solution was then filtered and 166 μl (1/6 volume) of dichloroethane was added. The solution was left for slow evaporation for 24 hours and then left at 5 °C for several days, where bright green irregularly shaped crystals suitable for X-ray diffraction were obtained. To obtain a crystalline phase-pure bulk sample of NiPd2 a filtered solution with a concentration of 0.0682 mM of [Ni(Pd(SAc)$_4$)(pyNO$_2$)] was gently heated to dryness over open flame. Yield: 32 % based on Pd. Elemental analysis calculated for $Pd_2Ni_2C_{26}H_{32}N_4O_{12}S_8$: C; 26.5 %, H; 2.74 %, N; 4.75 %. Found: C; 26.7 %, H; 2.85 %, N; 4.79 %.

[Co(Pt(SAc)$_4$)(pyNO$_2$)]$_2$, **{CoPt}$_2$**, 30 mg (0.0524 mmol) of [Co(Pt(SAc)$_4$)(OH$_2$)] was suspended in a mixture of 1 ml acetone and 10 ml CH_2Cl_2. To the suspension, a solution of 65 mg (0.524 mmol) 3-nitropyridine in a minimal amount of CH_2Cl_2 was added dropwise. The suspension was then stirred for 6 hours where the color of the filtrate changed from grayish to brown while the precipitate remained gray. The brown filtrate was isolated and carefully heated until dryness over open flame yielding brown block-shaped crystals suitable for X-ray diffraction experiments. Yield: 43 % based on Pt. Elemental analysis calculated for $Pt_2Co_2C_{26}H_{32}N_4O_{12}S_8$: C; 23.0 %, H; 2.38 %, N; 4.13 %. Found: C; 23.1 %, H; 2.40 %, N; 4.17 %.

[Ni(Pt(SAc)$_4$)(pyNO$_2$)]$_2$, **{NiPt}$_2$**, 30 mg (0.0524 mmol) of [Ni(Pt(SAc)$_4$)(OH$_2$)] was dissolved in 1 ml CH_2Cl_2 and dropwise adding a solution of 6.51 mg (0.0524 mmol) 3-nitropyridine in a minimal amount of CH_2Cl_2. The solution was then stirred for 1 hour. The remaining green solution was filtered and gently heated over open flame until a minimal amount of solvent remained. At this point the glassware was left at a cold surface were bright green block-shaped crystals were grown within an hour. Yield: 71 % based on Pt. Elemental analysis calculated for $Pt_2Ni_2C_{26}H_{32}N_4O_{12}S_8$: C; 23.0 %, H; 2.38 %, N; 4.13 %. Found: C; 23.1 %, H; 2.45 %, N; 4.20 %.

The complexes [Co(Pt(SAc)$_4$)(py)$_2$] and [Ni(Pt(SAc)$_4$)(py)$_2$] (**{CoPt}** and **{NiPt}**) were synthesized following previously reported procedures[2] and verified by powder X-ray diffraction.

[Co(Pd(SAc)$_4$)(py)$_2$], **{CoPd}**, 50 mg, 0.103 mmol [Co(Pd(SAc)$_4$)(OH$_2$)] was dissolved in 15 ml of pyridine. The solution was then gently heated over open flame and left on a cold surface and within the hour plank shaped brown crystal were grown in close to quantitative yield. Crystals suitable for X-ray diffraction experiments were grown by diluting the solution and prolonging crystallization time.

[Ni(Pd(SAc)$_4$)(py)$_2$], **{NiPd}**, was obtained in a similar fashion to the **{CoPd}** were the precursor was replaced with [Ni(Pd(SAc)$_4$)(OH$_2$)].
For both the synthesis of **{CoPd}** and **{NiPd}** the starting material could be replaced with dimerized complexes showing the greater affinity for the pyridine ligand.

[Ni(Pd(SAc)$_4$)(pyNO$_2$)], 33 mg (0.0682 mmol) of [Ni(Pd(SAc)$_4$)(OH$_2$)] was dissolved in 1 ml CH_2Cl_2 and dropwised adding, a solution of 8.47 mg (0.0682 mmol) 3-nitropyridine in a minimal amount of CH_2Cl_2. The solution was then stirred for 1 hour with a resulting change of color from yellow to bright green. The solution was then filtered and left for evaporation at room temperature. Bright green plank-shaped crystals were grown over the course of 24 hours and were suitable for X-ray diffraction experiments. Yield: 40 % based on Pd. Elemental analysis calculated for $PdNiC_{13}H_{16}N_2O_6S_4$: C; 26.5 %, H; 2.74 %, N; 4.75 %. Found: C; 26.9 %, H; 2.70 %, N; 4.95 %.

[Co(Pd(SAc)$_4$)(pyNO$_2$)], 33.0 mg (0.0682 mmol) [Co(Pd(SAc)$_4$)(OH$_2$)] was dissolved in 5 ml CH_2Cl_2 and diluted with 10 ml of ethanol. With rapid stirring a solution of 8.47 mg (0.0682 mmol) 3-nitropyridine in a minimal amount of CH_2Cl_2, was added dropwise. The solution was stirred for 24 hours at RT resulting in a color change from green to dark yellow. After 24 hours the solution was left for evaporation at room temperature where brown crystals suitable for X-ray diffraction experiments were grown. Yield: 54 % based on Pd. Elemental analysis calculated for $PdCoC_{13}H_{16}N_2O_6S_4$: C; 26.5 %, H; 2.73 %, N; 4.75 %. Found: C; 26.8 %, H; 2.69 %, N; 4.80 %.

The complexes [Co(Pd(SAc)$_4$)(pyNO$_2$)] and [Ni(Pd(SAc)$_4$)(pyNO$_2$)] are both a phase pure monomeric structure with the axial NO_2py ligand, but this type of monomer was never observed for the Pt analogs. Therefore, to have optimal comparability across the series only the iso-structural bis pyridine complexes are discussed in the paper and only the synthesis of the NO_2py Pd monomers is reported.

2 Single Crystal X-ray diffraction

Single crystal X-ray diffraction data were collected on a Bruker D8 VENTURE diffractometer equipped with a Mo Kα X-ray ($\lambda = 0.71073$ Å), and a PHOTON 100 CMOS detector. For low temperature measurements the diffractometer is equipped with an Oxford Cryosystem. All crystals were mounted on capton loops with a small amount of silicone grease. The data reductions were performed in the APEX3 software, and the absorption correction was carried out with the multi-scan method SADABS. The data collections were done at either 120 K or 100 K. The structures were solved in the Olex2 (ver. 1.3) software with the ShelXT software package included.
New structures presented in this work are found Figure S1-S4 and the crystallographic parameters can be found in Tables S1 and S2.

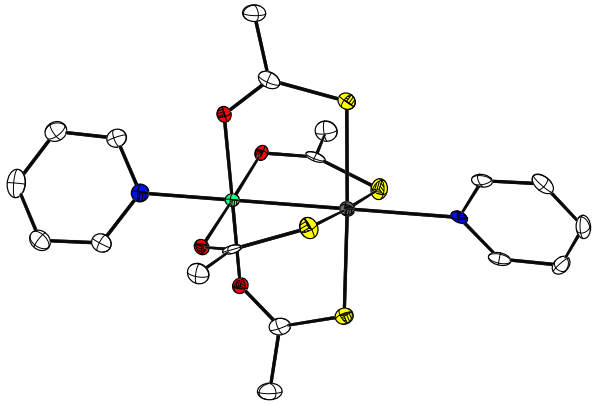

Figure S1: ORTEP representation of the crystal structure of **{NiPd}**, with 50 % probability ellipsoid. Hydrogen atoms are omitted for clarity. Color code: White: Carbon, red: Oxygen, blue: Nitrogen, yellow: Sulphur, grey: Palladium and aquamarine: Nickel.

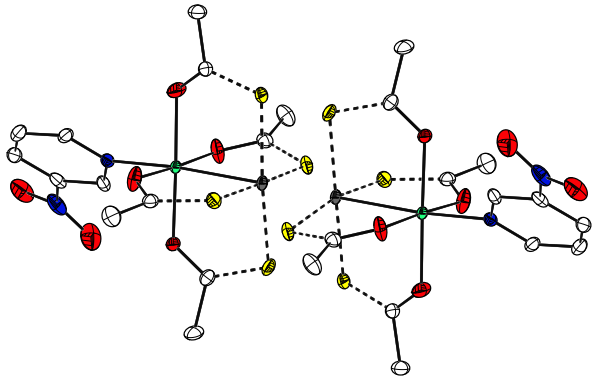

Figure S2: ORTEP representation of the crystal structure of **{NiPd}$_2$**, with 50 % probability ellipsoid. Hydrogen atoms as well as disordered sulphur atoms are omitted for clarity. Color code: White: Carbon, red: Oxygen, blue: Nitrogen, yellow: Sulphur, grey: Palladium and aquamarine: Nickel.

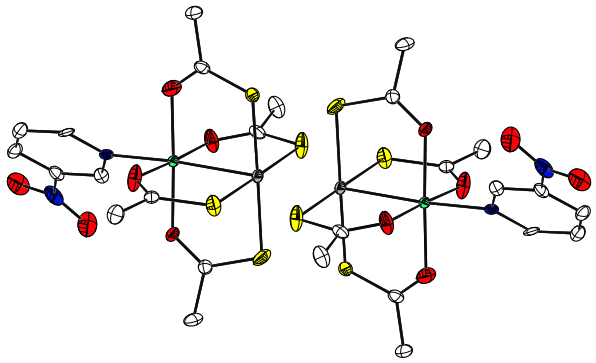

Figure S3: ORTEP representation of the crystal structure of $\mathbf{\{NiPt\}_2}$, with 50 % probability ellipsoid. Hydrogen atoms are omitted for clarity. Color code: White: Carbon, red: Oxygen, blue: Nitrogen, yellow: Sulphur, light grey: Platinum and aquamarine: Nickel.

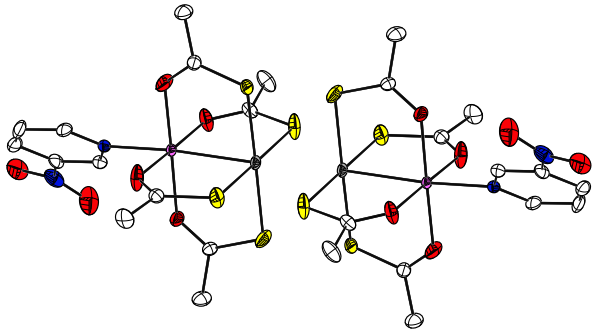

Figure S4: ORTEP representation of the crystal structure of $\mathbf{\{CoPt\}_2}$, with 50 % probability ellipsoid. Hydrogen atoms are omitted for clarity. Color code: White: Carbon, red: Oxygen, blue: Nitrogen, yellow: Sulphur, light grey: Platinum and lightpurple: Cobalt.

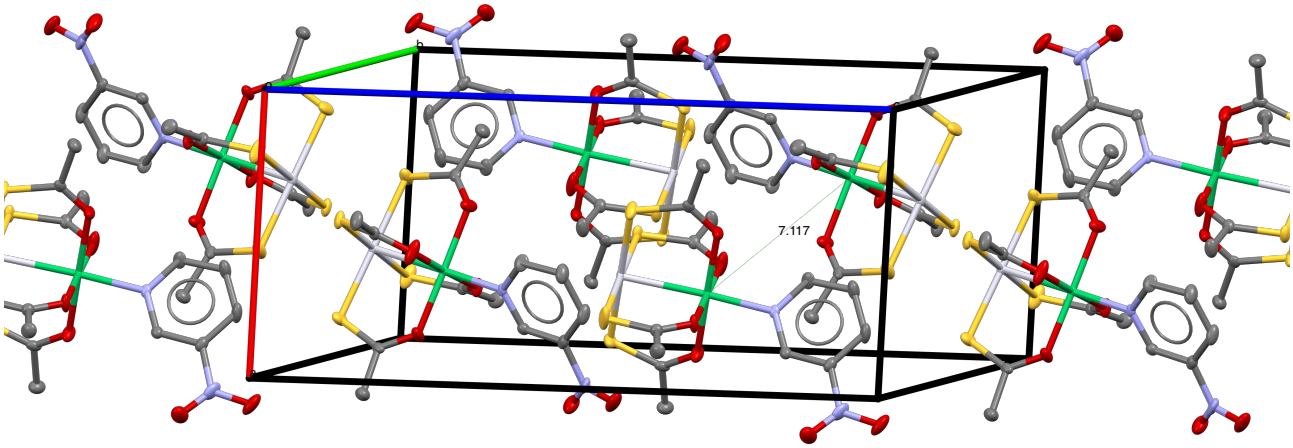

Figure S5: ORTEP representation of the crystal structure of $\mathbf{\{NiPt\}_2}$ showing the crystal packing with nearest neighbor at 7.1 Å. With 50 % probability ellipsoid and hydrogen atoms are omitted for clarity. Color code: White: Carbon, red: Oxygen, blue: Nitrogen, yellow: Sulphur, light grey: Platinum and aquamarine: Nickel.

Table S1: Crystallographic parameters

Compound	**{CoPd}**	**{CoPd}$_2$**	**{NiPd}**
Formula	$C_{18}H_{22}N_2CoO_4PdS_4$	$C_{13}H_{16}CoN_2O_6PdS_4$	$C_{18}H_{22}N_2NiO_4PdS_4$
Formula weight [g/mol]	623.94	589.8	623.72
Crystal system	Monoclinic	Monoclinic	Monoclinic
Space group	C 2/c	P 2_1/c	C 2/c
a / Å	9.7593(7)	8.4837	9.7142(7)
b / Å	18.2739(12)	12.3085(7)	18.2617(16)
c / Å	13.1854(8)	19.8273(11)	13.1518(12)
α / deg	90	90	90
β / deg	97.317(2)	93.171(2)	97.378
γ / deg	90	90	90
V / Å^3	2332.3(3)	2062.36(19)	2313.8
Z	4	4	4
ρ / g cm^{-3}	1.777	1.900	1.791
μ / mm^{-1}	1.867	2.112	1.979
Temperature / K	100	120	100
Radiation		Mo Kα (λ = 0.71073 Å)	
Crystal size / mm	0.251 x 0.186 x 0.126	0.488 x 0.223 x 0.156	0.282 x 0.055 x 0.049
2θ range / deg	4.458 to 61.012	5.282 to 67.608	2.46 to 50.048
Reflection collected	23760	88501	15895
Unique reflections	3562	8243	2050
R_{int}/R_σ	0.0496/0.0351	0.0372/0.0206	0.0972/0.0502
Parameters/restraints	141/0	248/0	141/0
Goodness of fit	1.029	1.069	1.021
R_1/wR_2 (I$\geq$2σ(I))	0.0287/0.0514	0.0325/0.0693	0.0321/0.0546
R_1/wR_2 (all data)	0.0431/0.0555	0.0430/0.0747	0.0546/0.0598
$\Delta\rho_{max}/\Delta\rho_{min}$ / e Å^{-3}	0.70/-0.66	1.59/-1.65	0.44/-0.52

Table S2: Crystallographic parameters continued, *identical to previously published

Compound	$\mathbf{\{NiPd\}_2}$	$\mathbf{\{CoPt\}_2}$ *	$\mathbf{\{NiPt\}_2}$
Formula	$C_{13}H_{16}NiN_2O_6PdS_{4.03}$	$C_{13}H_{16}CoN_2O_6PtS_4$	$C_{13}H_{16}NiN_2O_6PtS_4$
Formula weight [g/mol]	590.5	678.5	678.3
Crystal system	Monoclinic	Monoclinic	Monoclinic
Space group	P 2_1/c	P 2_1/c	P 2_1/c
a / Å	8.4953(6)	8.4704(10)	8.4782(4)
b / Å	12.3011(9)	12.2809(13)	12.2733(5)
c / Å	19.6004(14)	19.820(2)	19.6523(8)
α / deg	90	90	90
β / deg	92.680	93.914	93.668(2)
γ / deg	90	90	90
V / Å^3	2046.0(3)	2057.0(4)	2040.74(15)
Z	4	4	4
ρ / g cm^{-3}	1.917	2.191	2.208
μ / mm^{-1}	2.242	8.037	8.211
Temperature / K	100	100	100
Radiation		Mo Kα (λ = 0.71073 Å)	
Crystal size / mm	0.262 x 0.153 x 0.101	0.182 x 0.132 x 0.121	0.310 x 0.205 x 0.145
2θ range / deg	3.91 to 51.354	4.82 to 55.754	3.914 to 52.044
Reflection collected	30344	43264	26515
Unique reflections	3882	4899	3998
R_{int}/R_σ	0.0890/0.0442	0.0678/0.0341	0.0919/0.0559
Parameters/restraints	268/0	248/0	248/0
Goodness of fit	1.011	1.037	1.016
R_1/wR_2 (I$\geq$2σ(I))	0.0192/0.0410	0.0226/0.0391	0.0318/0.0637
R_1/wR_2 (all data)	0.0454/0.0639	0.0330/0.0417	0.0465/0.0686
$\Delta\rho_{max}/\Delta\rho_{min}$ / e Å^{-3}	0.73/-0.99	0.60/-0.81	0.98/-1.70

3 Powder X-ray diffraction

The Powder X-ray diffraction data were collected on a Bruker D8 ADVANCE powder diffractometer equipped with a Cu Kα X-ray source (λ = 1.5418 Å).

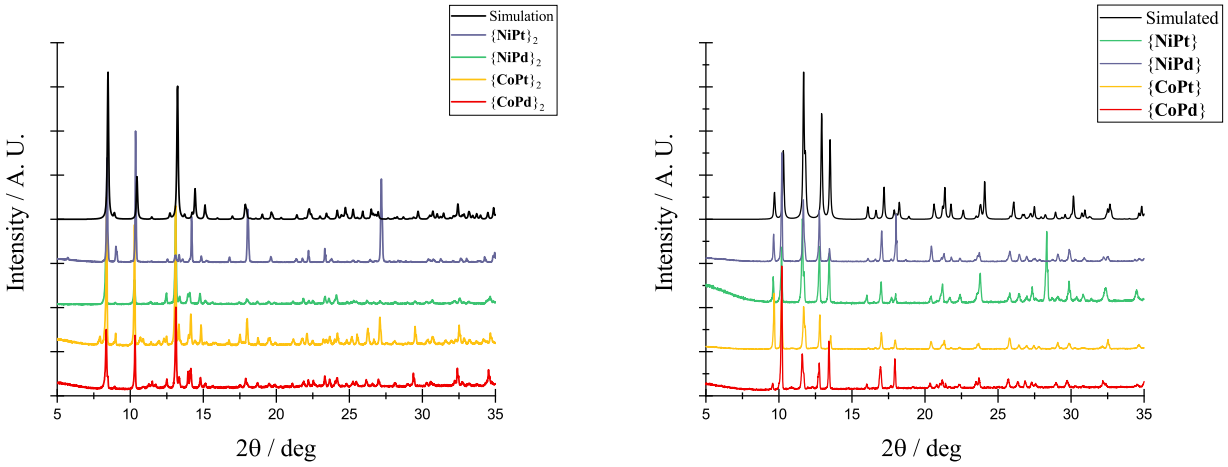

(a) (b)

Figure S6: Powder X-ray diffraction of (a) dimerized structures compared to a simulated structure and (b) monomeric structures compared to a simulated structure.

4 Calculated Energy Levels

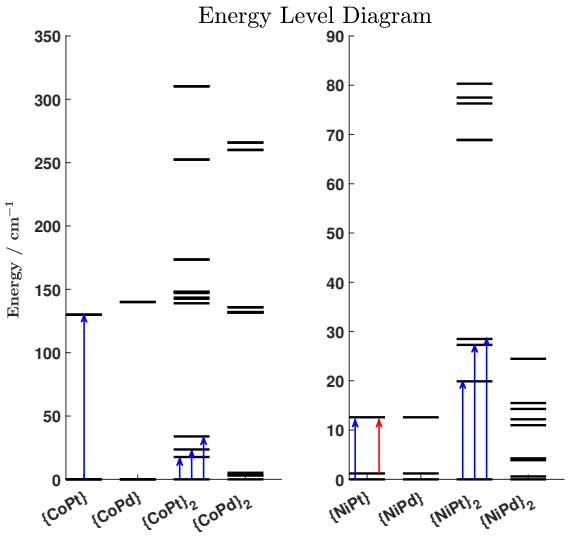

Figure S7: Calculated energy level diagram simulated from fitted parameters. Arrows indicate observed INS transitions, with blue representing transitions from the ground state and red from the first excited state.

5 Inelastic Neutron Scattering

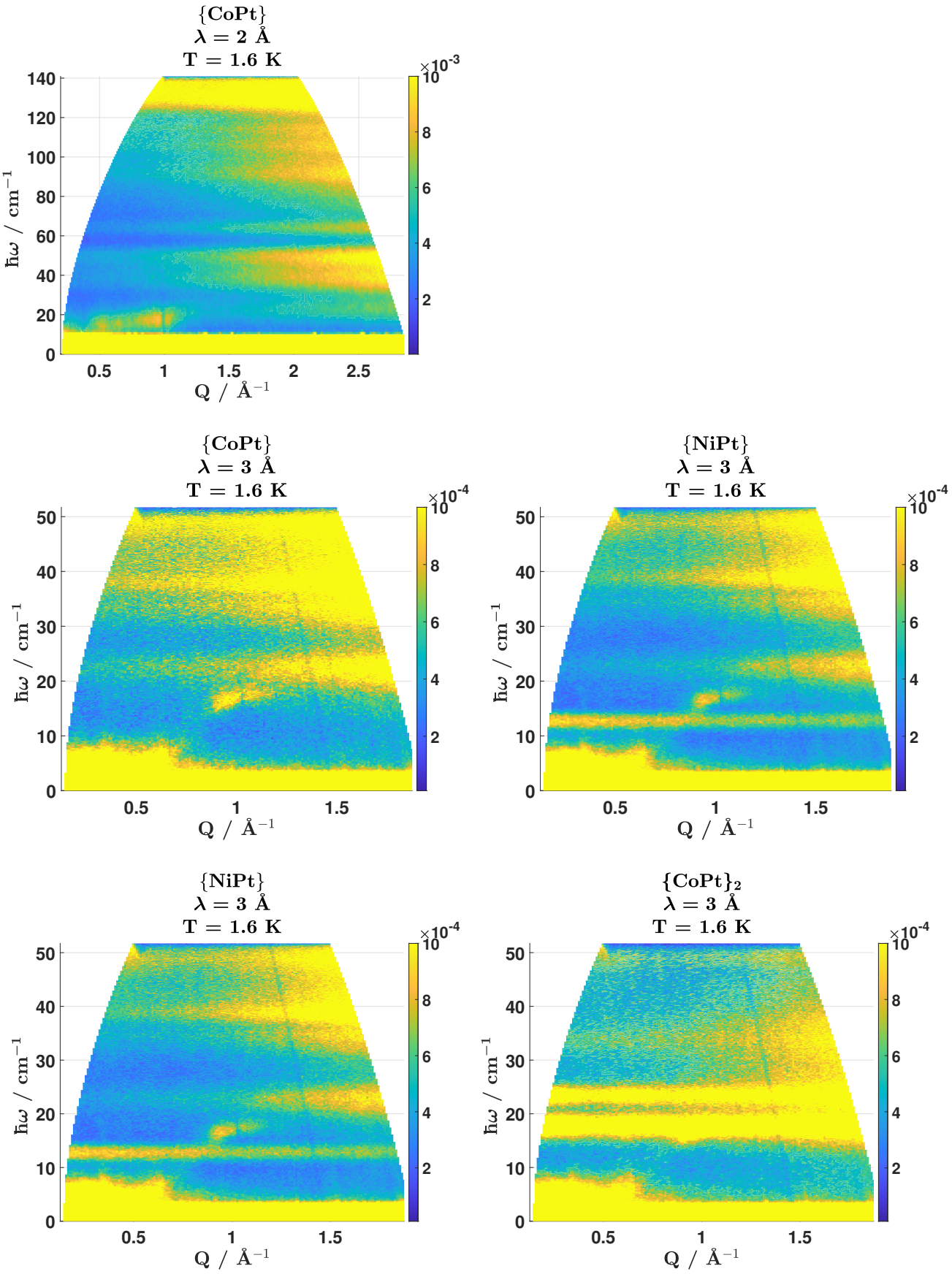

Figure S8: S(Q,ω) plots (neutron energy loss/) at 1.6 K. **{CoPt}** was measured at λ = 2 and 3 Å, whereas **{CoPt}$_2$**, **{NiPt}**, and **{NiPt}$_2$** were only measured at λ = 3 Å. A spurion is present at Q = 1 Å^{-1} and $\hbar\omega$ = 18 cm^{-1}.

6 FD-FT THz-EPR Spectroscopy

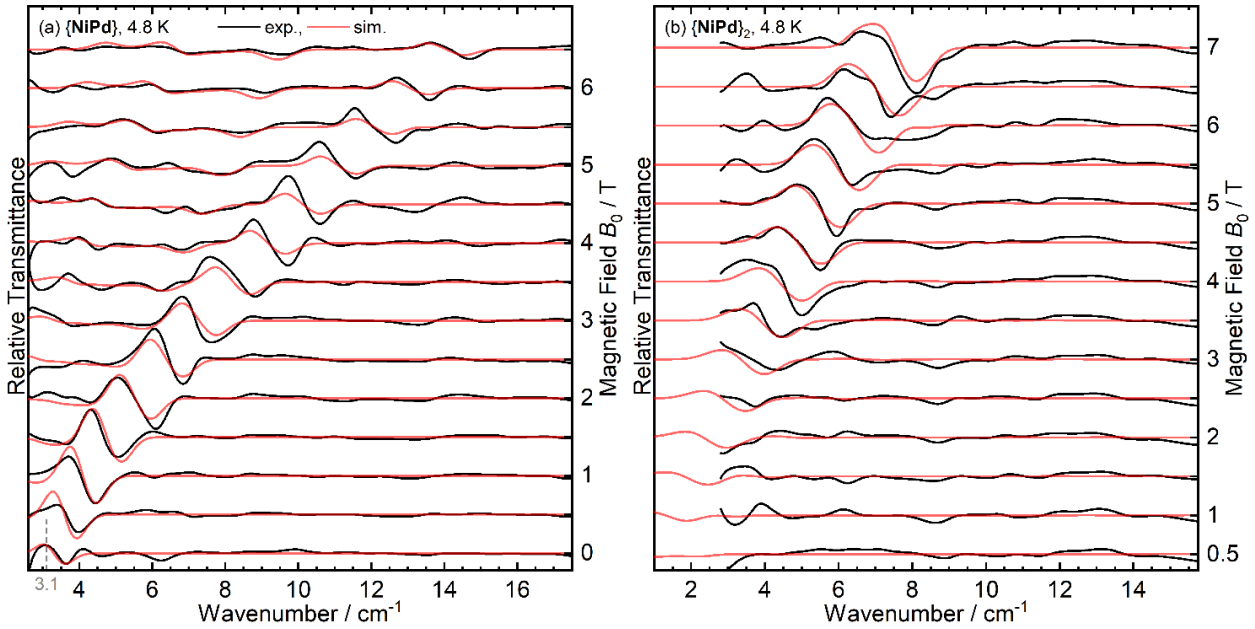

Figure S9: Experimental (black) and simulated (red) FD-FT THz-EPR magnetic-field division spectra of (a) **{NiPd}** and of (b) $\mathbf{\{NiPd\}_2}$ recorded at $T = 4.8$ K. Spectra were calculated by division of a transmission spectrum at $B_0 + 0.5$ T by a corresponding one at B_0. Thus, maxima correspond to stronger absorption at B_0, minima to increased absorption at the higher field.

FD-FT THz-EPR alone is capable of giving a parametrization of **{NiPt}**, $\mathbf{\{NiPt\}_2}$, **{NiPd}**, and $\mathbf{\{NiPd\}_2}$ which is found to be in accordance with the values found by SQUID magnetometry and INS. The following is a discussion on the extraction of parameters exclusively from THz.

Spectral simulations afford on-site Ni^{2+} parameters $D = -7.7$ cm^{-1} and $|E| = 0.4$ cm^{-1}, and with a fixed $J = 24.5$ cm^{-1} reproduce the temperature-dependent signal intensities very precisely (Simulations with variable J provide a fitted value of 21.8 cm^{-1}, which is in very good agreement with INS considering the S/N of the THz-EPR spectra). For the Pd^{2+}-containing compounds **{NiPd}** and $\mathbf{\{NiPd\}_2}$, two major differences are found compared to the Pt^{2+}-containing ones. (i) The signals are found at substantially lower transition energies. For **{NiPd}**, the zero-field peak is at 3.1 cm^{-1}, the lower edge of the experimentally accessible range, and appears unsplit. For $\mathbf{\{NiPd\}_2}$, the zero-field transitions are even located below the accessible energies, yet simulations of the field-dependency still allow to extract the Ni^{2+} ZFS parameters. With $D = -2.6$ cm^{-1} and $|E| = 0.6$ cm^{-1} for **{NiPd}** and $D = -0.9$ cm^{-1} and $|E| = 0.17$ cm^{-1} for $\mathbf{\{NiPd\}_2}$, it is apparent that D is substantially lower than in the corresponding Pt^{2+}-containing complexes, while the rhombicity is systematically larger. Furthermore, it is seen that the ZFS is larger in both monomers as compared to the dimers. (ii) The second major difference is that in contrast to $\mathbf{\{NiPt\}_2}$, $\mathbf{\{NiPd\}_2}$ signals are readily detectable at temperatures as low as 4.8 K already, consistent with a significantly smaller exchange interaction on the order of the thermal energy and confirmed by the simulations with a fixed $J = 5.0$ cm^{-1}.

Table S3: Optimized spin-Hamiltonian parameters from simulations of the FD-THz-EPR spectra.[a]

Compound	**{NiPt}**	$\mathbf{\{NiPt\}_2}$	**{NiPd}**	$\mathbf{\{NiPd\}_2}$
g	2.19	2.18	2.18	2.20
D / cm^{-1}	-12.3	-7.7	-2.6	-0.9
$\|E\|$ / cm^{-1}	0.6	0.4	0.6	0.17
$\|E\| / \|D\|$	0.05	0.05	0.23	0.18
J / cm^{-1}	-	21.8	-	5.0[b]

[a] *D and E are the on-site Ni^{2+} ZFS parameters.* [b] *Kept fixed during optimization.*

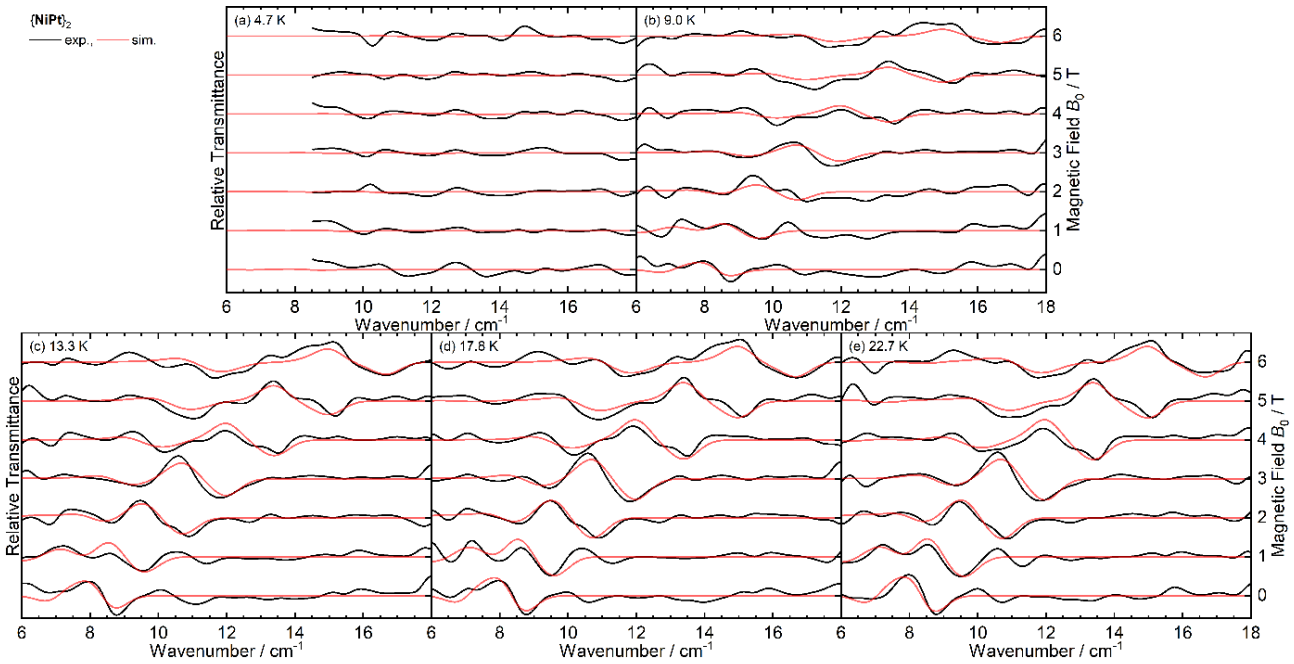

Figure S10: Experimental (black) and simulated (red) FD-FT THz-EPR magnetic-field division spectra of $\mathbf{\{NiPt\}_2}$ recorded at $T =$ (a) 4.7, (b) 9.0, (c) 13.3, (d) 17.8, and (e) 22.7 K. Spectra were calculated by division of a transmission spectrum at $B_0 + 1\,\mathrm{T}$ by a corresponding one at B_0. Thus, maxima correspond to stronger absorption at B_0, minima to increased absorption at the higher field. In (a), overly noisy data in the region $< 8.5\ \mathrm{cm}^{-1}$ due to the use of a different beam splitter (23 μm instead of 125 μm) are not shown.

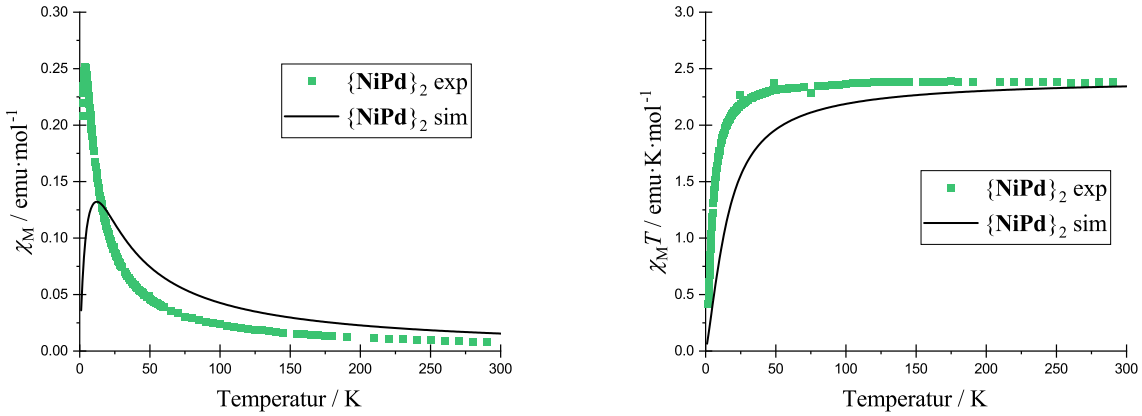

(a) (b)

Figure S11: (a) Magnetic susceptibility, χ_M, and (b) $\chi_M T$ of $\mathbf{\{NiPd\}_2}$ compared with a simulation with the parameters extracted from THz-EPR spectroscopy.

References

[1] F. G. Baddour, A. S. Hyre, J. L. Guillet, D. Pascual, J. M. Lopez-De-Luzuriaga, T. M. Alam, J. W. Bacon and L. H. Doerrer, *Inorganic Chemistry*, 2017, **56**, 452–469.

[2] F. G. Baddour, S. R. Fiedler, M. P. Shores, J. W. Bacon, J. A. Golen, A. L. Rheingold and L. H. Doerrer, *Inorganic Chemistry*, 2013, **52**, 13562–13575.